

NUMERICAL STUDY ABOUT TENSION PROPERTIES OF NOVEL HIERARCHICAL REENTRANT HONEYCOMB STRUCTURE

Dongquan WU^{1*}, Zhenyi XU¹, Zhuo YUAN¹, Yupeng LI¹, Zixiang LIU¹, Zhiqiang ZHANG²

¹ Sino-European Institute of Aviation Engineering, Civil Aviation University of China, Tianjin, China

² Institute of Aviation Engineering, Civil Aviation University of China, Tianjin, China

*corresponding author, dqwu@cauc.edu.cn

This study designed and analyzed three novel hierarchical reentrant honeycomb structures, composed of nested subunits with varying Poisson's ratio characteristics, to evaluate their tensile performance through simulations and experiments. The results show that all three structures exhibit the negative Poisson's ratio under tensile loading in both axial directions, with the subunits' Poisson's ratios influencing the overall Poisson's ratio of the structure. The CH structure demonstrates higher stiffness under Y -axis loading, while the SRH structure exhibits higher stiffness under X -axis loading. In terms of deformation, the CH structure shows greater flexibility compared to the other two. The SRH structure consistently maintains an intermediate tensile strength among the three.

Keywords: reentrant structure; hierarchical; Poisson's ratio; tension performance.



Articles in JTAM are published under Creative Commons Attribution 4.0 International.
Unported License <https://creativecommons.org/licenses/by/4.0/deed.en>.
By submitting an article for publication, the authors consent to the grant of the said license.

Nomenclature of abbreviation

- RH – novel hierarchical reentrant honeycomb structures with reentrant honeycomb subunit,
- SRH – novel hierarchical reentrant honeycomb structures with semi-reentrant honeycomb subunit,
- CH – novel hierarchical reentrant honeycomb structures with classic hexagonal honeycomb subunit.

1. Introduction

The rapid development of aerospace (Heo *et al.*, 2013; Gong *et al.*, 2022; Solak *et al.*, 2023) and military industries has driven a significant demand for lightweight materials with superior mechanical properties (Wang, 2019). Among these, various honeycomb structures, which have shown great potential, have been extensively studied and applied. These structures can be designed to exhibit excellent performance in stiffness, strength, impact resistance, and energy absorption. It is well known that the key to achieving such outstanding mechanical behavior lies in the design of the structural topology. Based on this, researchers have developed honeycomb structures with various geometries, including hexagonal, Kagome (Liu *et al.*, 2021), circular (Ahmed & Xue, 2019), and triangular shapes.

Unlike traditional hexagonal honeycomb structures, reentrant honeycomb structures are characterized by inward-curved cell designs on both sides, providing excellent shear resistance and energy absorption properties. Additionally, reentrant honeycomb structures exhibit the unique property of the negative Poisson's ratio. This means that under axial tensile loading, the cross-section of the reentrant honeycomb structure expands, while under axial compression, the cross-section contracts. This characteristic endows reentrant honeycomb structures with significantly better macroscopic mechanical properties compared to traditional lattice structures (Photiou *et al.*, 2016) or foam materials (Köhnen *et al.*, 2018), such as superior dent resistance during elastic deformation (Patel *et al.*, 2018), higher shear modulus (Ju & Summers, 2011),

enhanced dynamic dent resistance during plastic yield (Hu *et al.*, 2019), and greater energy absorption capacity (Xiao *et al.*, 2019a; Jin *et al.*, 2016). Previous studies have explored these properties in depth: Boldrin *et al.* (2016) discussed the dynamic behavior of negative Poisson's ratio honeycombs and found that specific gradient topologies are highly sensitive to dynamic performance. Xiao *et al.* (2019b), through experimental analysis, examined the compressive behavior of reentrant honeycombs and identified V and I deformation modes. Liu *et al.* (2016) investigated the energy absorption of reentrant honeycombs, claiming that due to early densification, reentrant honeycombs absorb more energy than traditional honeycombs under the same compressive strain. Lee *et al.* (2019) elaborated on the crushing performance of reentrant honeycomb structures, including crushing stress and energy absorption.

However, all the design concepts mentioned above are limited to single-layer honeycomb structures, which have low in-plane stiffness and fail to meet the increasingly stringent requirements of engineering applications, thus limiting their potential use. Research by Chen *et al.* (2018) has shown that complex hierarchical structures are key to achieving high specific stiffness, specific strength, and energy absorption efficiency. This design is inspired by various natural organisms, such as bones (Liu *et al.*, 2022), shells, and bamboo (Reznikov *et al.*, 2018), which exhibit hierarchical structures at multiple scales, with each scale corresponding to the next. These biological materials achieve exceptional mechanical properties through their complex layered structures. The introduction of hierarchical structures can enhance the strength, toughness, and durability of materials. The interaction between layers allows the material to better distribute and absorb stress under external forces, thereby improving the overall mechanical performance of the structure.

While previous studies have extensively explored hierarchical and reentrant honeycomb structures, a significant research gap remains in understanding the tensile performance of novel hierarchical reentrant honeycomb structures. This study developed three new types of hierarchical reentrant honeycomb structures by incorporating honeycomb subunits with different Poisson's ratios and replacing the traditional cell walls with a double-layer nested configuration. Experimental and simulation methods were employed to investigate the tensile performance of these structures in two directions, with numerical comparisons made for elastic modulus, Poisson's ratio, fracture strain, and tensile strength. The deformation characteristics were also analyzed and summarized. The results indicate that these newly designed honeycomb structures effectively utilize hierarchical configurations to enhance the dynamic tensile behavior of honeycomb structures. This study offers insights and references for designing multifunctional lightweight structures with tailored Poisson's ratios.

2. Structure design and method

In this study, reentrant honeycomb structures with a negative Poisson's ratio, semi-reentrant honeycomb structures with the zero Poisson's ratio, and classical hexagonal honeycomb structures with the positive Poisson's ratio were employed as subunits. Unlike traditional hierarchical honeycomb structures, a novel double-layer nested configuration was introduced to replace the conventional cell walls of reentrant honeycomb structures. The detailed structural design is shown in Fig. 1. In order to facilitate the comparison and analysis of the subsequent simulation results, the dimensions of the three novel hierarchical reentrant honeycomb structures designed in this study are controlled at $c = 142$ mm long and $b = 87$ mm wide, and the cell wall thickness of all three cellular metamaterials $t = 0.6$ mm and a thickness of this substructure is 5 mm. Meanwhile, the detailed geometrical definition for the dimensions of the substructure is carried out in this study. The reentrant honeycomb subunit with negative Poisson's ratio (Shukla & Behera, 2022), the reentrant honeycomb substructure designed in this study has a wall length $h = 4$ mm, $l = 1.8$ mm, a turning angle $\beta = 33.69^\circ$; and for the semi-reentrant honeycomb subunit with zero Poisson's ratio (Xiao *et al.*, 2019b; Ingrole *et al.*, 2017) designed in this study

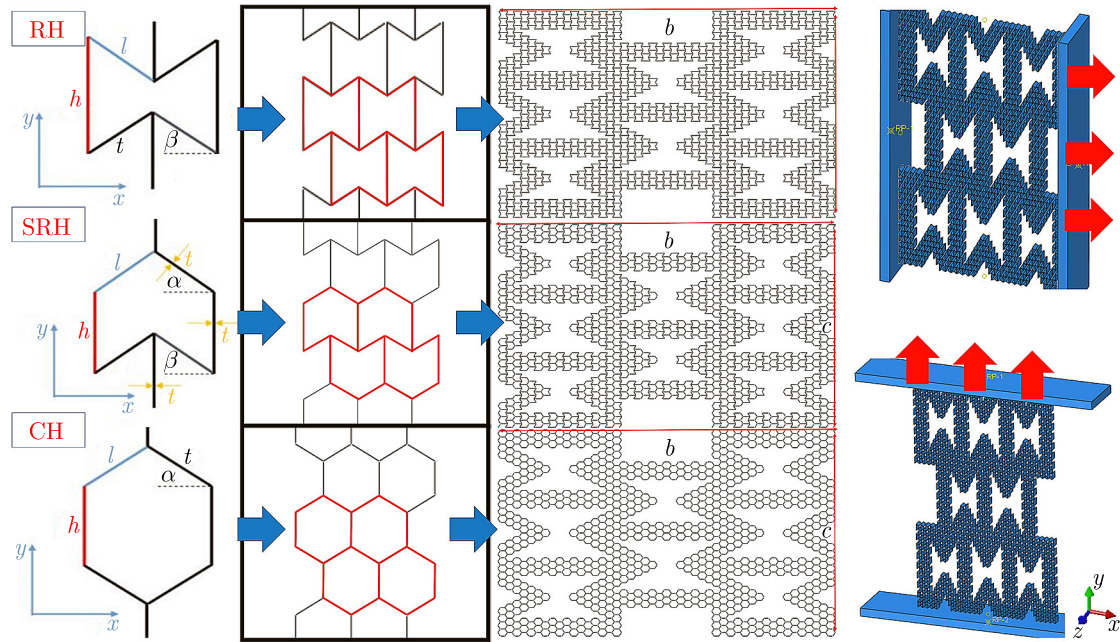


Fig. 1. Three novel hierarchical reentrant honeycomb structures and simulation.

has a wall length $h = 3$ mm, $l = 1.8$ mm, a turning angle $\alpha = \beta = 33.69^\circ$. For the classical hexagonal honeycomb subunit which is positive Poisson's ratio (Xu *et al.*, 2024), the honeycomb wall length $h = 2$ mm, $l = 1.8$ mm, a turning angle $\alpha = 33.69^\circ$.

This paper evaluates the tensile performance of three novel hierarchical reentrant honeycomb structures using the finite element analysis and tensile simulations conducted with Abaqus 2023. Additionally, tensile experiments were performed on 3D-printed samples produced with fused deposition modeling (FDM) technology to comprehensively assess the tensile properties of these structures. The tensile performance was examined in two directions.

In the finite element simulations, rigid plates were attached to both sides of the honeycomb structures. Axial displacement boundary conditions corresponding to the tensile direction were applied on one side, while fixed support boundary conditions were set on the opposite side. The simulation used a “dynamic/explicit” analysis step, with a friction coefficient of 0.3 applied tangentially, and a “hard contact”, general contact setting applied in the normal direction. The honeycomb structures were meshed using S4R (four-node shell) elements with a mesh size of 2, while the plates were meshed using C3D8R (eight-node linear hexahedral) elements with a mesh size of 4. In total, the honeycomb structures consisted of approximately 90,000 mesh elements.

For the experimental analysis, the study included the hierarchical reentrant honeycomb structure designed by scholar Lian, referred to as RH1, to compare mechanical properties. To maintain scientific validity, the overall configuration and wall thickness were kept constant, with minor adjustments to the structure's dimensions to match the frame length of the structures designed in this study. All samples were fabricated using fused deposition modeling (FDM) 3D printing technology under consistent parameters: a printing temperature of 210°C , a bed temperature of 40°C , and a layer orientation angle of 0° . To analyze deformation behavior during tensile testing, a digital image correlation (DIC) system was used to capture precise deformation morphologies at specific tensile strains, with images recorded every 4 seconds. Tensile tests were conducted using a universal testing machine at a constant rate of 2 mm/min, as shown in Fig. 2.

The material used in this simulation analysis is polylactic acid (PLA), a biodegradable polymer prepared from renewable resources. The specific material property parameters used in the simulation are shown in Table 1.

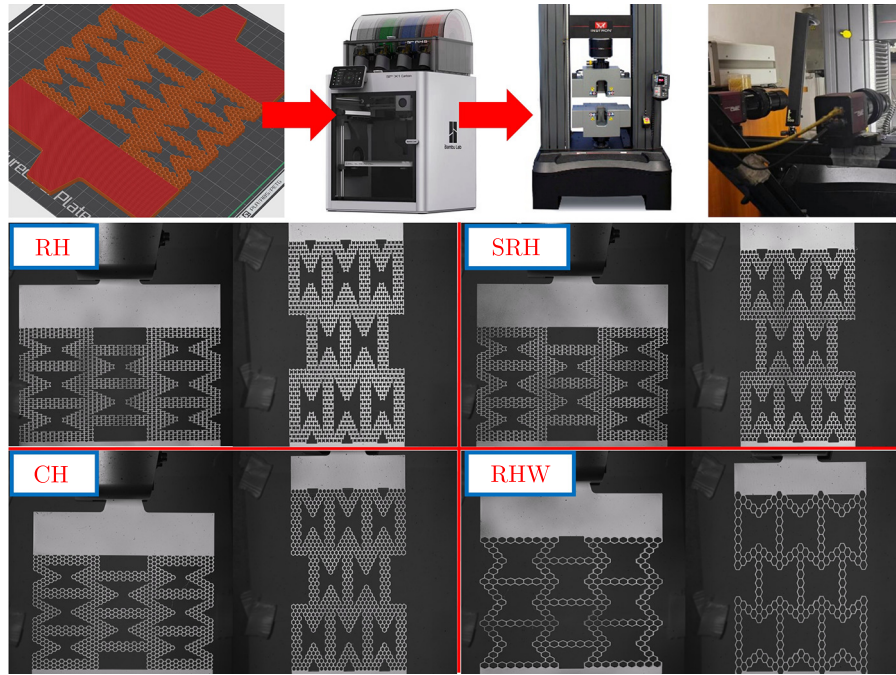


Fig. 2. Experiments on 3D printed solids under FDM

Table 1. Mechanical properties of PLA.

Materials	Elastic modulus [MPa]	Yield strength [MPa]	Fracture strain	Poisson's ratio	Mass density ρ_A [kg/m ³]
PLA	2500	39.14	0.18	0.3	1378

3. Simulation of bi-directional tensile simulation

3.1. Simulation of stretching along the X -axis

As shown in Fig. 3, deformation characteristics were captured at tensile strains of 0.05, 0.10, 0.15, and 0.20. A comprehensive analysis revealed significant differences in the fracture strain of the three structures: RH fractured below 0.05, SRH between 0.05 and 0.10, and CH between 0.10 and 0.15. Notably, the fracture locations were similar across all three structures, occurring at the junctions of the hierarchical substructures, specifically in the central honeycomb subunits. This is due to the central honeycomb structure being more prone to deformation, as it is subjected to the combined effects of surrounding structures and vertical layers. As tensile strain increases, fractures extend from the center toward the outer regions of the structure. Additionally, at a tensile strain of 0.2, deformation occurs primarily in the middle layer, with the upper and lower hierarchical honeycomb layers remaining largely undeformed. This suggests that the novel hierarchical reentrant honeycomb structure has a unique ability to protect the outer layers during axial tensile loading as shown in Fig. 3.

Stress values are determined by dividing reaction forces (F) from the rigid grip section by the cross-sectional area of the grip section (S). Therefore, stress is represented as σ_1 or $\sigma_2 = F/S$. Strains ($\varepsilon = U/d$) are derived from the ratio of top grip displacements (U) to the structure's length (d). Poisson's ratio is defined as $\nu = -\varepsilon_v/\varepsilon$, where ε_v is the strain perpendicular to the axial load direction and ε is the axial strain value, the stress-strain curve plotted against Poisson's ratio-strain curve obtained is shown in Fig. 4.

The tensile stress-strain curve in Fig. 4a depicts the progression from initial tensile loading to the first fracture in the structure. The curve reveals that all three structures undergo an

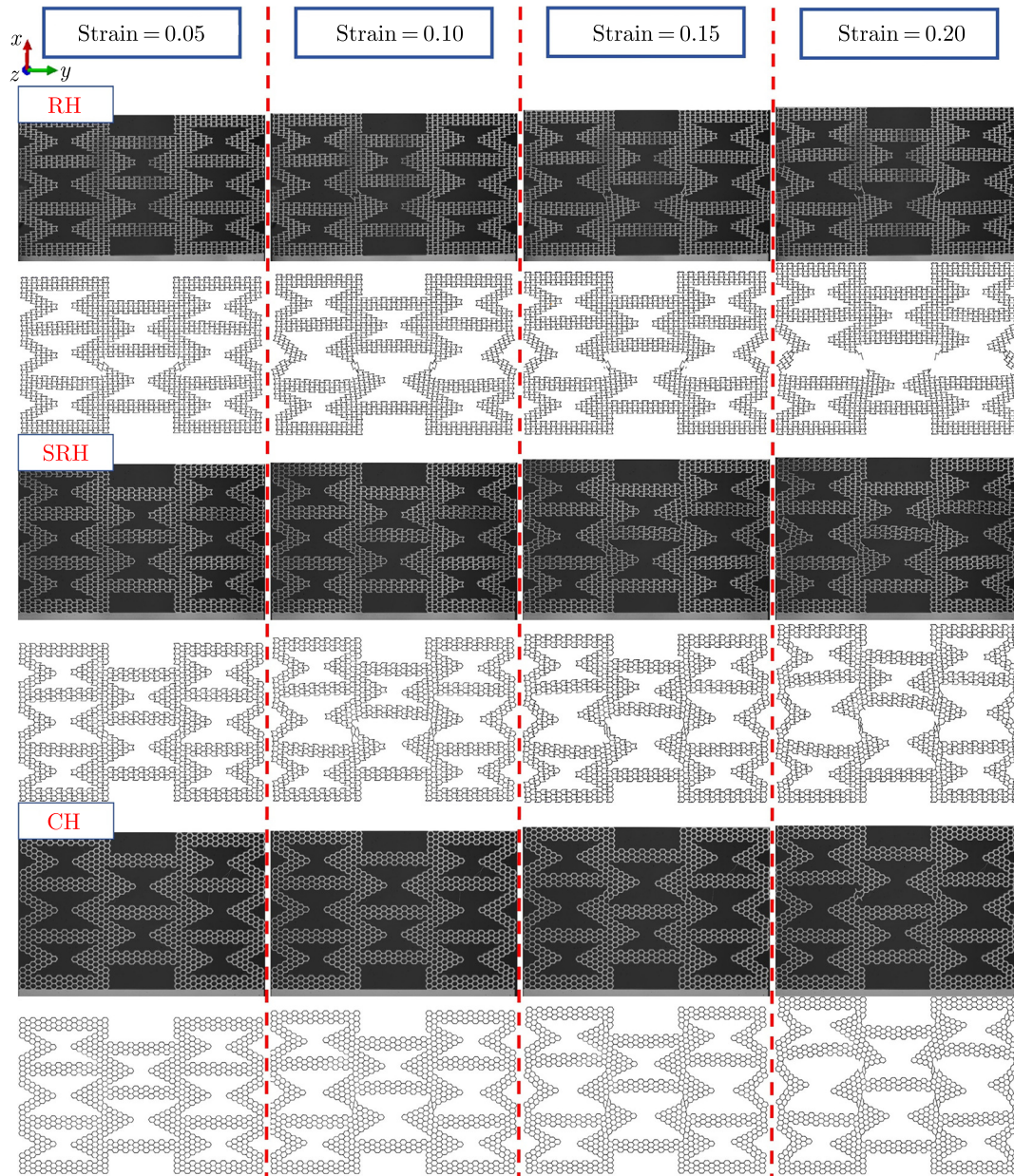


Fig. 3. Characteristics of tensile deformation along X-axis.

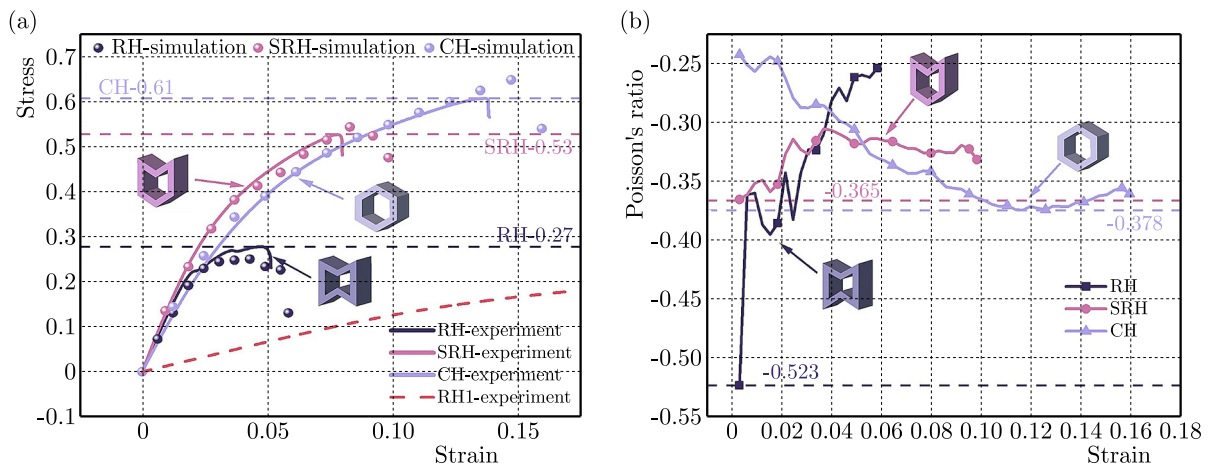


Fig. 4. Tensile stress-strain curves and Poisson's ratio-strain curves along the X-axis.

initial elastic phase, a buckling phase, and a final fracture during the tensile test. By applying Hooke's Law to the initial elastic phase, the elastic moduli of the three different structures can be calculated. The figure also shows the tensile strength of each structure at the fracture strain, with specific data provided in Table 2. The study results indicate that, in terms of the elastic modulus, $SRH > RH > CH$, suggesting that the SRH structure has greater stiffness and stability compared to the other two. This is because the semi-reentrant honeycomb subunits in the SRH structure combine the mechanical properties of the other two subunits, resulting in stronger interactions during tensile loading.

Table 2. Physical parameters related to stretching along the X -axis.

Type	Elastic modulus [MPa]	Rupture strain	Tensile strength [MPa]	Minimum Poisson's ratio
RH	12.68	0.05	0.27	-0.523
SRH	13.93	0.08	0.53	-0.365
CH	10.41	0.14	0.61	-0.378

However, in terms of tensile strength, the order is $CH > SRH > RH$. Despite having a lower elastic modulus, the CH structure's deformation characteristics allow it to undergo greater deformation during tensile loading. This increased deformation helps the CH structure disperse stress concentrations more effectively and absorb more energy before fracturing, resulting in superior tensile strength. On the other hand, the SRH and RH structures tend to transfer energy through fracture rather than significant deformation. As a result, they fracture under lower stress, leading to a relatively lower tensile strength. The SRH structure, which combines characteristics of both subunits, has a tensile strength between the other two. The RH structure, due to its earlier fracture strain, fractures earlier in the tensile process, exhibiting the lowest tensile strength among the three.

Additionally, when examining the RH1 structure individually, it is evident from the images that the novel hierarchical reentrant honeycomb structure designed in this study has a significantly higher elastic modulus compared to the RH1 structure. This suggests that the structure developed in this research offers greater stability.

As shown in Fig. 4b, all three structures exhibit negative Poisson's ratio characteristics during tensile loading up to the first fracture. However, Poisson's ratio trends differ: the RH and SRH structures show an overall increase, while the CH structure shows a decrease. The study also found that the RH structure has the smallest minimum Poisson's ratio among the three, with SRH and CH having relatively similar values. This phenomenon can be attributed to the inherent negative Poisson's ratio of the reentrant honeycomb subunits, which directly influences the overall Poisson's ratio of the RH structure. This observation further supports the conclusion that Poisson's ratio of the subunits directly impacts Poisson's ratio of the entire structure. Additionally, the tensile study under out-of-plane compression along the X -axis confirmed the alignment between the simulation results and the physical experiments.

3.2. Simulation of stretching along the Y -axis

During tensile loading along the Y -axis, deformation images were captured at four strain nodes: 0.05, 0.1, 0.15, and 0.2, as shown in Fig. 5. The results indicate that at a tensile strain of 0.15, the RH and SRH structures exhibited significant fractures, while the CH structure fractured at a tensile strain of 0.2. The fracture points for SRH and RH were located at the junctions of the hierarchical structures, with RH's fracture occurring on the walls of the middle hierarchical structure. These findings suggest that the CH structure has superior flexibility during tensile loading, consistent with the results from the X -axis tensile tests. Further analysis revealed that the reentrant and semi-reentrant honeycomb subunits did not undergo significant deformation;

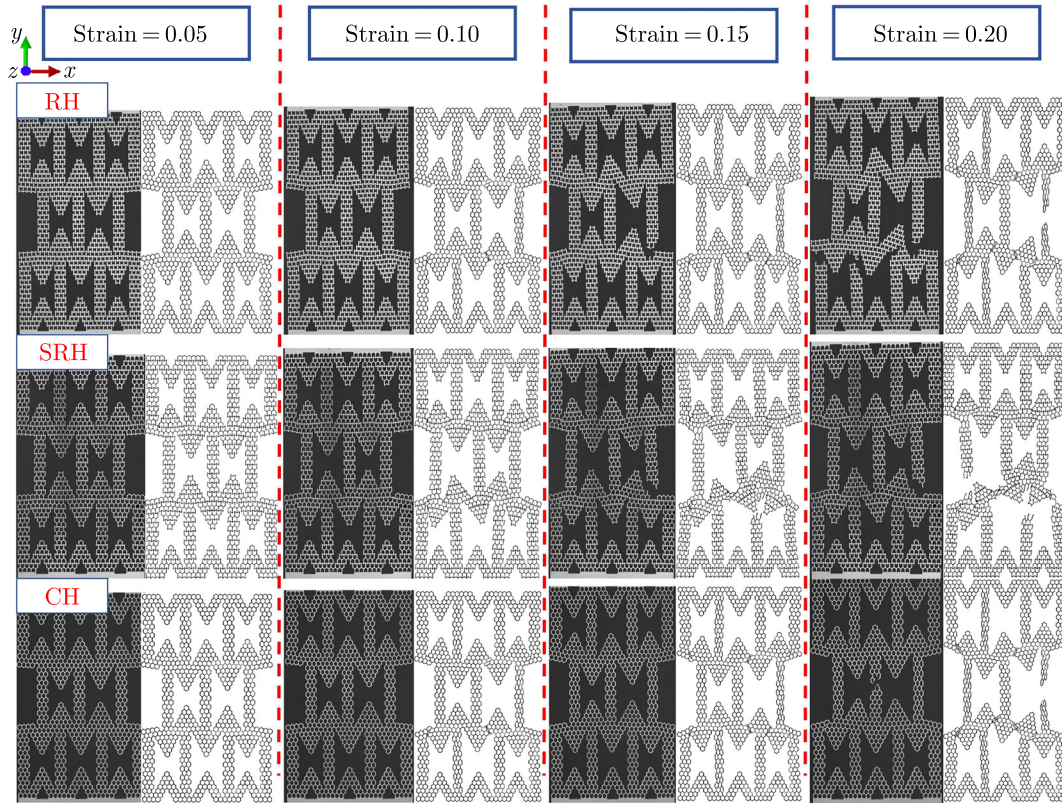


Fig. 5. Characteristics of tensile deformation along Y-axis.

instead, the energy of the structure was released through fracturing. In contrast, the classical hexagonal honeycomb subunits experienced greater deformation during tensile loading, which helped to distribute stress more evenly and delayed fracture, resulting in a later fracture point. Notably, the RH and SRH structures exhibited an outside-in fracture pattern, while the CH structure showed an inside-out fracture pattern.

Figure 6 shows the stress-strain and Poisson’s ratio-strain curves for tensile loading along the Y-axis, with detailed mechanical properties presented in Table 3. Compared to the tensile data under X-axis loading (Table 2), the results reveal that the elastic moduli of all three structures are significantly higher under Y-axis loading. This is because, during Y-axis tensile loading, the axial tensile direction is parallel to the sidewalls of the hierarchical reentrant honeycomb

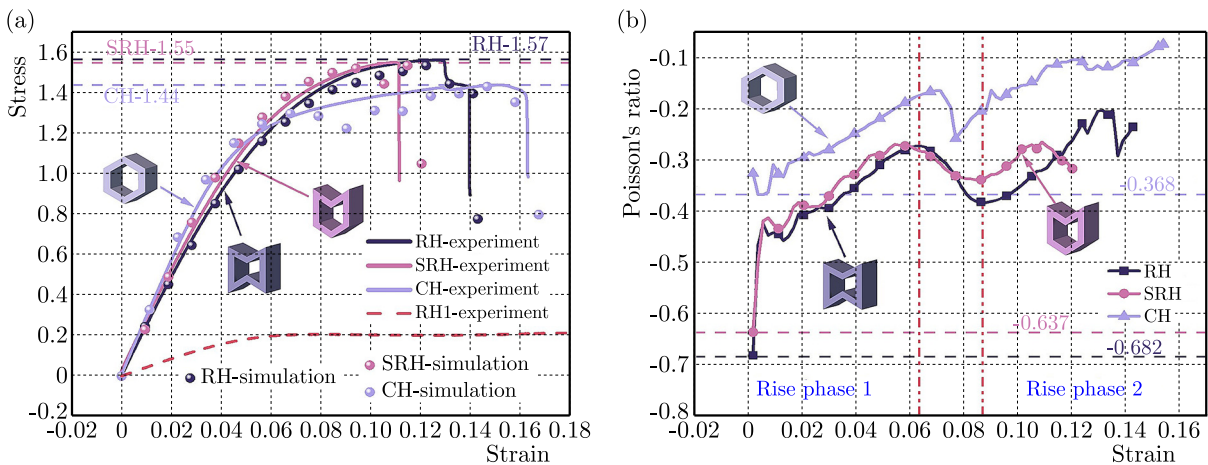


Fig. 6. Tensile stress-strain curves and Poisson’s ratio-strain curves along the Y-axis.

Table 3. Physical parameters related to stretching along the X -axis.

Type	Elastic modulus [MPa]	Rupture strain	Tensile strength [MPa]	Minimum Poisson's ratio
RH	25.09	0.14	1.57	-0.682
SRH	25.54	0.11	1.55	-0.637
CH	28.91	0.16	1.44	-0.368

substructure, which provides greater stiffness and stability. However, the change in loading direction also alters the stiffness characterization. Under Y -axis tensile loading, the stiffness ranking is $CH > SRH > RH$. For fracture strain, the order is $CH > RH > SRH$, likely due to the unique flexibility of the classical hexagonal honeycomb structure. In terms of tensile strength, the order is $RH > SRH > CH$, with the values for SRH and RH being relatively close. The analysis of the curves suggests that the lower tensile strength of the CH structure is due to its extended yielding phase. Furthermore, the comparison of the simulation and experimental curves in Fig. 6a confirmed the alignment between the experimental results and simulations. Additionally, when comparing the RH1 structure based on experimental data, it was observed that the novel hierarchical reentrant honeycomb structures designed in this study generally exhibit higher stiffness and stability.

The analysis of Poisson's ratio characterization in different structures, as shown in Fig. 6b, reveals that Poisson's ratio-strain curves under Y -axis tensile loading not only exhibit a fully negative Poisson's ratio, but all three structures also display two distinct increasing phases, specifically in the strain intervals of 0–0.06 and 0.086–0.15. To further quantify the negative Poisson's ratio characteristics, the minimum Poisson's ratio is ranked as $RH < SRH < CH$, indicating that the RH structure has the most optimal negative Poisson's ratio under Y -axis tensile loading. This conclusion is consistent with the findings from tensile loading along the X -axis, further confirming that Poisson's ratio of the subunits significantly influences the overall Poisson's ratio of the structure. Additionally, the results suggest that the change in axial tensile direction has a relatively small impact on Poisson's ratio characteristics.

4. Conclusion

This study designed three novel hierarchical reentrant honeycomb structures by nesting various subunits to replace the cell walls of traditional reentrant honeycomb structures. The mechanical behavior of these structures under axial tensile loading in two directions was evaluated using the finite element analysis and tensile testing of 3D-printed samples.

In terms of elastic modulus, under X -axis tensile loading, the SRH structure exhibited the highest stiffness, followed by the RH and CH structures. However, under Y -axis tensile loading, the CH structure demonstrated superior stiffness, indicating its robustness and stability in this direction. Compared to RH1 designed by Lian, the structures in this study exhibited higher stiffness and stability, even with similar dimensions. Regarding tensile strength, under X -axis loading, the CH structure displayed the highest tensile strength, attributed to its ability to undergo greater deformation, which aids in the stress distribution. Conversely, under Y -axis loading, the RH structure exhibited the highest tensile strength, followed by the SRH and CH structures. The study of deformation morphology revealed significant differences in fracture patterns across different loading directions. The RH and SRH structures tended to fracture earlier, exhibiting an outside-in fracture mode in both loading directions, whereas the CH structure fractured later, showing an inside-out fracture mode, indicating its greater flexibility. In terms of Poisson's ratio, all three structures exhibited the consistent negative Poisson's ratio under tensile loading, with the RH structure showing the most pronounced effect. This consistency in both loading directions indicates that Poisson's ratio of the subunits significantly influences

the overall Poisson's ratio of the hierarchical structure. This study offers valuable insights for designing multifunctional lightweight materials with tailored mechanical properties.

Acknowledgments

The authors would like to acknowledge the support from the Fundamental Research Funds for the Central Universities (grant no. 3122024041) and the Graduate Research Innovation Program of Civil Aviation University of China (grant no. 2023YJSKC12002).

References

1. Ahmed, N. & Xue, P. (2019). Governing the in-plane axial crushing of honeycomb with regular hexagonal symmetric division cells using cross-hinge inserts. *International Journal of Mechanical Sciences*, 161–162, Article 105062. <https://doi.org/10.1016/j.ijmecsci.2019.105062>
2. Boldrin, L., Hummel, S., Scarpa, F., Di Maio, D., Lira, C., Ruzzene, M., Remillat, C.D.L., Lim, T.C., Rajasekaran, R., & Patsias, S. (2016). Dynamic behaviour of auxetic gradient composite hexagonal honeycombs. *Composite Structures*, 149, 114–124. <https://doi.org/10.1016/j.compstruct.2016.03.044>
3. Chen, Y., Li, T., Jia, Z., Scarpa, F., Yao, C.W., & Wang, L. (2018). 3D printed hierarchical honeycombs with shape integrity under large compressive deformations. *Materials & Design*, 137, 226–234. <https://doi.org/10.1016/j.matdes.2017.10.028>
4. Gong, X., Ren, C., Sun, J., Zhang, P., Du, L., & Xie, F. (2022). 3D Zero Poisson's Ratio honeycomb structure for morphing wing applications. *Biomimetics*, 7(4), 198. <https://doi.org/10.3390/biomimetics7040198>
5. Heo, H., Ju, J., & Kim, D.M. (2013). Compliant cellular structures: Application to a passive morphing airfoil. *Composite Structures*, 106, 560–569. <https://doi.org/10.1016/j.compstruct.2013.07.013>
6. Hu, L.L., Zhou, M.Z., & Deng, H. (2019). Dynamic indentation of auxetic and non-auxetic honeycombs under large deformation. *Composite Structures*, 207, 323–330. <https://doi.org/10.1016/j.compstruct.2018.09.066>
7. Ingrole, A., Hao, A., & Liang, R. (2017). Design and modeling of auxetic and hybrid honeycomb structures for in-plane property enhancement. *Materials & Design*, 117, 72–83. <https://doi.org/10.1016/j.matdes.2016.12.067>
8. Jin, X., Wang, Z., Ning, J., Xiao, G., Liu, E., & Shu, X. (2016). Dynamic response of sandwich structures with graded auxetic honeycomb cores under blast loading. *Composites Part B: Engineering*, 106, 206–217. <https://doi.org/10.1016/j.compositesb.2016.09.037>
9. Ju, J. & Summers, J.D. (2011). Compliant hexagonal periodic lattice structures having both high shear strength and high shear strain. *Materials & Design*, 32(2), 512–524. <https://doi.org/10.1016/j.matdes.2010.08.029>
10. Köhnen, P., Haase, C., Bültmann, J., Ziegler, S., Schleifenbaum, J.H., & Bleck, W. (2018). Mechanical properties and deformation behavior of additively manufactured lattice structures of stainless steel. *Materials & Design*, 145, 205–217. <https://doi.org/10.1016/j.matdes.2018.02.062>
11. Lee, W., Jeong, Y., Yoo, J., Huh, H., Park, S.J., Park, S.H., & Yoon, J. (2019). Effect of auxetic structures on crash behavior of cylindrical tube. *Composite Structures*, 208, 836–846. <https://doi.org/10.1016/j.compstruct.2018.10.068>
12. Liu, H., Zhang, E.T., Wang, G., & Ng, B.F. (2022). In-plane crushing behavior and energy absorption of a novel graded honeycomb from hierarchical architecture. *International Journal of Mechanical Sciences*, 221, Article 107202. <https://doi.org/10.1016/j.ijmecsci.2022.107202>
13. Liu, J., Chen, W., Hao, H., & Wang, Z. (2021). In-plane crushing behaviors of hexagonal honeycombs with different Poisson's ratio induced by topological diversity. *Thin-Walled Structures*, 159, Article 107223. <https://doi.org/10.1016/j.tws.2020.107223>
14. Liu, W., Wang, N., Luo, T., & Lin, Z. (2016). In-plane dynamic crushing of re-entrant auxetic cellular structure. *Materials & Design*, 100, 84–91. <https://doi.org/10.1016/j.matdes.2016.03.086>

15. Patel, P., Bhingole, P.P., & Makwana, D. (2018). Manufacturing, characterization and applications of lightweight metallic foams for structural applications: Review. *Materials Today: Proceedings*, 5(9), 20391–20402. <https://doi.org/10.1016/j.matpr.2018.06.414>
16. Photiou, D., Prastiti, N., Sarris, E., & Constantinides, G. (2016). On the conical indentation response of elastic auxetic materials: Effects of Poisson's ratio, contact friction and cone angle. *International Journal of Solids and Structures*, 81, 33–42. <https://doi.org/10.1016/j.ijsolstr.2015.10.020>
17. Reznikov, N., Bilton, M., Lari, L., Stevens, M.M., & Kröger, R. (2018). Fractal-like hierarchical organization of bone begins at the nanoscale. *Science*, 360(6388), Article eaao2189. <https://doi.org/10.1126/science.aao2189>
18. Shukla, S. & Behera, B.K. (2022). Auxetic fibrous structures and their composites: A review. *Composite Structures*, 290, Article 115530. <https://doi.org/10.1016/j.compstruct.2022.115530>
19. Solak, A., Aşçıoğlu Temiztaş, B., & Bolat, B. (2023). Numerical investigation of the mechanical behavior of the vertical stabilizer leading edge with wavy honeycomb sandwich structure under bird strike. *Journal of Sandwich Structures & Materials*, 25(3), 387–400. <https://doi.org/10.1177/10996362221146124>
20. Wang, Z. (2019). Recent advances in novel metallic honeycomb structure. *Composites Part B: Engineering*, 166, 731–741. <https://doi.org/10.1016/j.compositesb.2019.02.011>
21. Xiao, D., Chen, X., Li, Y., Wu, W., & Fang, D. (2019a). The structure response of sandwich beams with metallic auxetic honeycomb cores under localized impulsive loading-experiments and finite element analysis. *Materials & Design*, 176, Article 107840. <https://doi.org/10.1016/j.matdes.2019.107840>
22. Xiao, D., Dong, Z., Li, Y., Wu, W., & Fang, D. (2019b). Compression behavior of the graded metallic auxetic reentrant honeycomb: Experiment and finite element analysis. *Materials Science and Engineering: A*, 758, 163–171. <https://doi.org/10.1016/j.msea.2019.04.116>
23. Xu, P., Lan, X., Zeng, C., Zhang, X., Zhao, H., Leng, J., & Liu Y. (2024). Compression behavior of 4D printed metamaterials with various Poisson's ratios. *International Journal of Mechanical Sciences*, 264, Article 108819. <https://doi.org/10.1016/j.ijmecsci.2023.108819>

*Manuscript received February 21, 2024; accepted for publication October 18, 2024;
published online March 14, 2025.*